# Polymer Chemistry

Carbolong Chemistry

ROYAL SOCIETY
OF CHEMISTRY

**PAPER**
Jiangxi Chen, Haiping Xia *et al.*
Photothermal Möbius aromatic metallapentalenofuran and its
NIR-responsive copolymer

Check for updates

# Photothermal Möbius aromatic metallapentalenofuran and its NIR-responsive copolymer†

Zhengyu Lu,[a,b] Yuanting Cai,[b] Yuanqing Wei,[b] Qin Lin,[a] Jiangxi Chen, [iD] *[a] Xumin He,[b] Shunhua Li,[b] Weitai Wu [iD] [b] and Haiping Xia [iD] *[b]

Möbius aromatics are very interesting and rare complexes owing to their brand-new chemistry and interesting properties. In this work, metallapentalenofurans with thiophene groups were easily prepared from the reaction of metallapentalyne, terminal arylalkynes, and water in air. The metallapentalenofuran containing a terthiophene moiety showed a good photothermal effect and was the first photothermal Möbius aromatic complex induced by *J*-aggregates. This photothermal metallapentalenofuran was chemically modified to carry an olefinic group and then was co-polymerized with oligo-(ethylene glycol)methacrylate to afford a thermoresponsive copolymer, whose phase transition behavior can be triggered by near-infrared radiation at 808 nm. This near-infrared-responsive metal-containing copolymer represents a new stimuli-responsive macromolecule.

## Introduction

Coplanar Möbius aromatic organometallic complexes are very interesting and rare complexes owing to their brand-new chemistry in terms of structure and bonding.[1–4] Thanks to their highly conjugated system, they are expected to display interesting properties for light harvesting, light emission, energy transfer, *etc*. For example, we found that the Möbius aromatic complex **1** (Fig. 1) exhibits aggregation-enhanced near-infrared emission (AEE)[1] behavior. Complex **2** (Fig. 1) has been reported to display photoacoustic imaging properties when irradiated at 680 nm,[5] and complex **3** (Fig. 1) shows excellent photothermal effects when exposed to near-infrared (NIR) radiation at 808 nm.[3,6] Moreover, complex **3** was chemically modified to produce the first photothermal metal-containing macromolecule **4** (Fig. 1).[7]

It is noted that metallopolymers with organometallic building blocks are interesting and valuable materials, since they are expected to display properties of both organometallic and
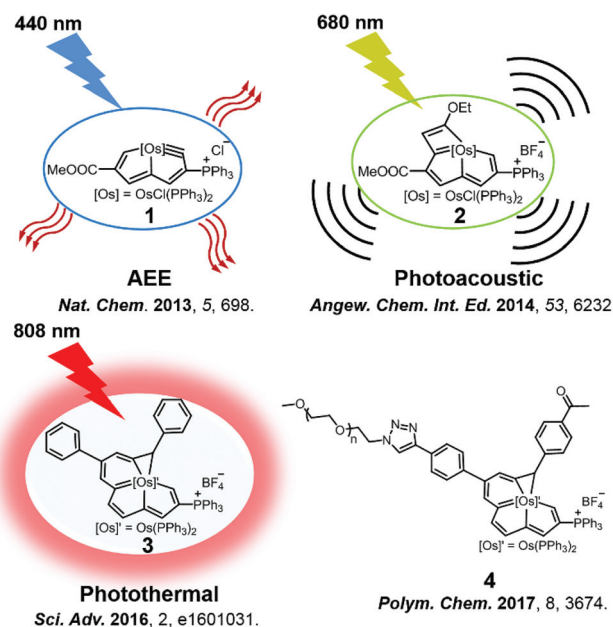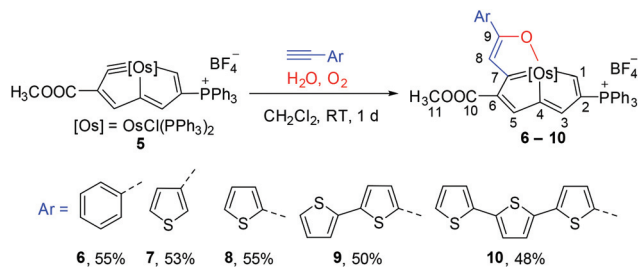


**Fig. 1** Möbius aromatic compounds with different properties.

polymeric units.[8–10] Metallopolymers have been developed as functional materials[11–21] to be applied in the field of catch and release,[22] electrodes,[23] optics,[24] ion capture,[25] water purification,[26] surface wettability,[27] self-healing,[28] electrocatalysts[29] or others.[30,31] A representative metallopolymer is polyferrocenylsilane, which has been developed as a stimuli responsive

*[a]Department of Materials Science and Engineering, College of Materials, Xiamen University, Xiamen 361005, People's Republic of China. E-mail: chenjx@xmu.edu.cn*
*[b]State Key Laboratory of Physical Chemistry of Solid Surfaces and Collaborative Innovation Center of Chemistry for Energy Materials (iChEM), College of Chemistry and Chemical Engineering, Xiamen University, Xiamen 361005, People's Republic of China. E-mail: hpxia@xmu.edu.cn*

**Scheme 1** Preparation of osmapentalenofurans **6–10** from osmapentalyne **5** and terminal aryl alkynes.
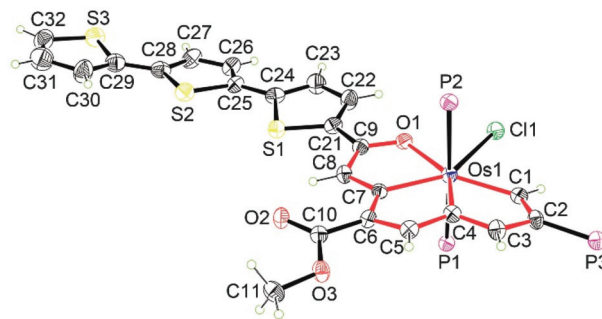


**Fig. 2** X-ray molecular structure for the cation of **10** (ellipsoid set at 50% probability). Phenyl groups in the PPh₃ groups are omitted for clarity. Selected bond lengths [Å] and angles [°]: Os1–C1 2.081(6), Os1–C4 2.139(6), Os1–C7 2.115(5), Os1–O1 2.130(4), C1–C2 1.367(8), C2–C3 1.423(8), C3–C4 1.377(8), C4–C5 1.393(8), C5–C6 1.356(7), C6–C7 1.436(7), C7–C8 1.394(7), C8–C9 1.398(7), C9–O1 1.289(7); Os1–C1–C2 124.4(4), C1–C2–C3 111.4(5), C2–C3–C4 112.1(5), C3–C4–Os1 121.2(4), C4–Os1–C1 70.7(2), Os1–C4–C5 120.9(4), C4–C5–C6 114.9(5), C5–C6–C7 111.2(5), C6–C7–Os1 122.0(4), C7–Os1–C4 70.8(2), Os1–C7–C8 116.8(4), C7–C8–C9 114.4(5), C8–C9–O1 115.4(5), C9–O1–Os1 120.1(3), O1–Os1–C7 73.14(18).

material/sensor[32,33] on the basis of its redox active properties and can even grow to a metallosupramolecular polymer *via* a living crystallization-driven self-assembly.[34–36] However, metallopolymers displaying photothermal properties are rare.[7]

In our continuous efforts to develop new metalla-aromatic[37–43] complexes, we have recently reported an easy route for the preparation of α-metallapentalenofurans from the reaction of complex **5** with terminal arylalkynes and water in air (Scheme 1).[4] Compared to air or moisture sensitive organometallic complexes using standard Schlenk techniques,[44] these metallapentalenofurans can be prepared under very mild conditions in good yield, which motivated us to develop them further into functional materials.

In this work, we report a new photothermal metallapentalenofuran, which is the first photothermal Möbius aromatic complex induced by *J*-aggregates. This metalla-aromatic complex was incorporated into a thermoresponsive copolymer, which phase transition can be triggered by an NIR laser at 808 nm. The resulted NIR-responsive metal-containing copolymer represents a new stimuli-responsive macromolecule.

## Results and discussion

### Synthesis of osmapentalenofurans 8–10 with (oligo)thiophen-5-yl groups

Recently, we have reported the reaction of osmapentalyne **5** with terminal arylalkynes and water to afford the first α-metallapentalenofurans (**6** and **7**).[4] Following this chemistry, a series of metallapentalenofurans (**8–10**) with thiophen-2-yl or oligothiophen-5-yl groups were easily synthesized by the treatment of osmapentyne **5** with different ethynylthiophenes (2-ethynylthiophene, 5-ethynyl-2,2′-bithiophene, or 5-ethynyl-2,2′:5′,2″-terthiophene) and water at room temperature (RT) for 1 day under an air atmosphere (Scheme 1).

Complexes **8–10** were characterized by nuclear magnetic resonance (NMR) spectroscopy, high-resolution mass spectra (HRMS), and elemental analysis (EA). Complexes **9** and **10** were also characterized by X-ray diffraction analysis. As shown in Fig. S23† (**9**) and Fig. 2 (**10**), the structures of **9** and **10** are similar to that of complex **6** except that they contain 2,2′-bithiophen-5-yl and 2,2′:5′,2″-terthiophen-5-yl moieties. The three fused five-membered rings formed by atoms Os1, O1,

and C1–C9 are approximately coplanar, as reflected by the mean deviations from the least-squares plane (0.067 Å for **9** and 0.108 Å for **10**). All Os–C bond lengths in the metallacycles (Os1–C1 2.091, Os1–C4 2.138, Os1–C7 2.129 Å for **9** and Os1–C1 2.081, Os1–C4 2.139, Os1–C7 2.115 Å for **10**) are in the range of those for reported osmapentalenes (1.926–2.175 Å).[2,37] The C–C bond lengths (1.348–1.440 Å for **9** and 1.356–1.436 Å for **10**) of the three fused five-membered rings are between those of C–C and C=C bond lengths. All the structural features indicate that the metallacycles in complexes **9** and **10** are also delocalized, as in the case of the reported osmapentalenofuran **6**.

The NMR data of **8–10** are consistent with the solid-state structure. In particular, the ³¹P{¹H} NMR spectra show two signals: the C*P*Ph₃ signals appear at 10.75 ppm for **8**, 10.79 ppm for **9**, and 10.81 ppm for **10**, the two equivalent Os*P*Ph₃ signals appear at −17.38 ppm for **8**, −17.41 ppm for **9**, and −17.42 ppm for **10**. The characteristic OsC*H* signal appears at 13.75 ppm for **8**, 13.72 ppm for **9**, and 13.73 ppm for **10**. These results confirm that the structures of complexes **8–10** are similar to those of complexes **6** and **7**.

### UV-Vis-NIR absorption spectra and photothermal properties

The UV-Vis-NIR absorption behavior of these highly conjugated metal-containing polycyclic complexes (**7–10**) is shown in Fig. 3. In the visible region, the maximum absorption bands of **7–10** are located at 572, 581, 597, and 605 nm, respectively. It is understandable that the red shift of the maximum absorption and the increase of the molar extinction coefficient are related to the increasing number of substituted thiophene units.

To our surprise, complex **10** with the 2,2′:5′,2″-terthiophen-5-yl group was found to exhibit a new broad absorption band
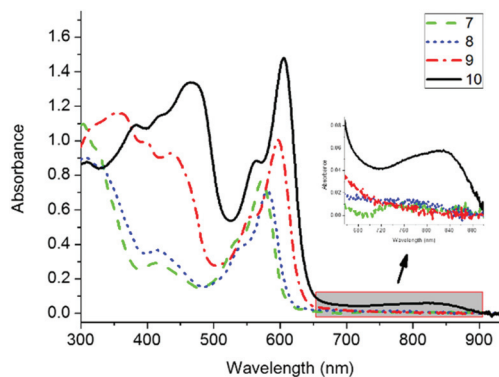
**Fig. 3** UV-Vis-NIR absorption spectra of **7**, **8**, **9**, and **10** ($5.0 \times 10^{-5}$ mol L$^{-1}$) measured in CH$_2$Cl$_2$ at RT.



**Fig. 5** (a) UV-Vis-NIR absorption spectra of CH$_2$Cl$_2$ solutions of **10** at different concentrations (2.0, 4.0, 6.0, 8.0, and $10.0 \times 10^{-5}$ mol L$^{-1}$) at RT. (b) Molar absorption coefficient ($\varepsilon$) of different concentrations of **10** (2.0, 4.0, 6.0, 8.0, and $10.0 \times 10^{-5}$ mol L$^{-1}$) at 823 nm.

covering the range of 700–900 nm. Its absorption pattern and intensity are very similar to those of complex **3**, which exhibits excellent photothermal behavior. Inspired by this result, we examined the photothermal properties of complex **10** by measuring the temperature of its solution under NIR laser irradiation (808 nm, 1.0 W cm$^{-2}$). As shown in Fig. 4, the temperature of a water–ethanol (1 : 9, v/v) solution of complex **10** quickly increased under 808 nm light irradiation. In particular, the solution containing 1.00 mg mL$^{-1}$ of complex **10** exhibited a rapid temperature increase from 28 to 57 °C within 5 min, while the solvent presented a negligible temperature change under similar conditions. These results suggest that complex **10** displays good photothermal properties.

To understand the observed absorption behavior, we performed time-dependent density functional theory (TD-DFT) calculations on complexes **8–10**. The main absorption bands dominated by HOMO → LUMO transitions were calculated to appear at 519, 545, and 568 nm for **8**, **9**, and **10**, respectively. The calculation results are consistent with the observed solution absorption behavior in the visible region ($\lambda_m = 581$ nm for **8**, $\lambda_m = 597$ nm for **9**, and $\lambda_m = 605$ nm for **10**). Unfortunately, no other calculated electron transition energies could be assigned to the broad and weak absorption band at
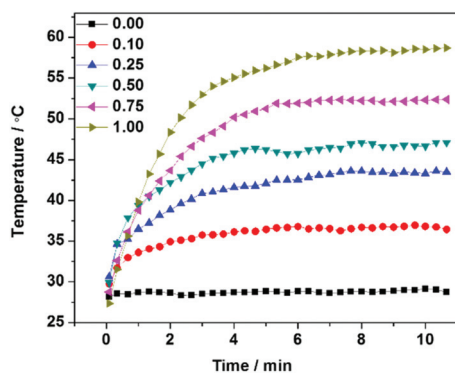
700–900 nm, even after analyzing the singlet and triplet states of complex **10**.

Compared to complexes **8** and **9**, complex **10** bears a larger 2,2′:5′,2″-terthiophen-5-yl group. Since such a larger coplanar group presents easy π–π stacking interactions leading to J-aggregates, the red-shift absorption of complex **10** could arise from said J-aggregates.[45–49] To confirm this hypothesis, we studied the spectral behavior of complex **10** at different concentrations, since aggregation processes are highly dependent on the concentration. As shown in Fig. 5, the increasing concentration of **10** resulted in increasing molar extinction coefficients at 823 nm, suggesting that the broad NIR absorption band of complex **10** is resulted from J-aggregates driven by π–π stacking of the 2,2′:5′,2″-terthiophen-5-yl side chain. It is noted that previously reported photothermal materials were nanoparticles caused by surface plasmon resonance[50–58] and compounds due to their highly conjugated structures.[58–62] There were only a few photothermal materials resulting from J-aggregates.[63–68] To the best of our knowledge, this is the first example of a Möbius aromatic complex with photothermal properties induced by J-aggregates, despite such J-aggregate phenomena being quite common.

The broad and weak absorption at 700–900 nm (Fig. 3) of complex **10** suggests that the aggregation behavior is weak. The spherical shape (see the crystal structure in Fig. 2) of the metal center in complex **10** may account for this weak aggregation: steric effects compete with the π–π stacking of the 2,2′:5′,2″-terthiophen-5-yl groups, leading to weak aggregation. For complexes **8** and **9**, the smaller thiophen-2-yl and 2,2′-bithiophen-5-yl side chains do not provide sufficient driving force (π–π stacking) to exhibit such aggregation behavior. Thus, complexes **8** and **9** do not present an absorption band at 700–900 nm induced by J-aggregates.

### Synthesis of osmapentalenofuran 12 with a methacrylate group

The successful preparation of the photothermal complex **10** inspired us to further develop it into a photothermal material. For this purpose, we introduced an olefinic group on the metalla-aromatic complex, since compounds with olefinic groups can be easily grown into macromolecules by radical polymerization.[69] The incorporation of **10** in a polymer may



**Fig. 4** Temperature curves of solutions of **10** in 90% water–ethanol (v/v) at different concentrations (0.00, 0.10, 0.25, 0.5, 0.75, and 1.00 mg mL$^{-1}$) irradiated with an 808 nm laser at a power density of 1.0 W cm$^{-2}$.
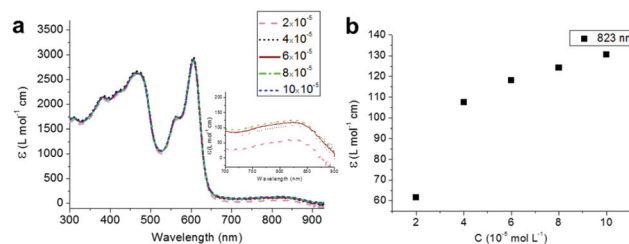
have two effects: first, it can improve the water-solubility and biocompatibility of complex **10**; secondly, it may improve to some extent the aggregation behavior of complex **10**.

Osmapentalynes with vinyl groups have been successfully prepared in our group.[70] Following this direction, treatment of olefinic osmapentalyne **11** with 5-ethynyl-2,2′:5′,2′-terthiophene and water at RT gave methacrylate osmapentalenofuran **12**. Complex **12** was characterized by NMR spectroscopy, HRMS, and EA. The $^{31}P\{^{1}H\}$ NMR spectrum of complex **12** shows two signals at 10.77 (C$PPh_3$) and −17.45 (Os$PPh_3$) ppm, while the $^{1}H$ NMR spectrum shows the characteristic OsC$H$ signal at 13.75 ppm. These results confirmed that the metallacyclic substructure of complex **12** is similar to that of complex **10**. In addition, the methacrylate group in complex **12** was confirmed by the signals at 6.23 (H15), 5.71 (H15), 4.36 (H12), 4.23 (H11), and 2.02 (H16) ppm in the $^{1}H$ NMR spectrum and at 167.2 (C13), 136.0 (C14), 126.5 (C15), 62.8 (C12), 61.9 (C11), and 18.5 (C16) ppm in the $^{13}C\{^{1}H\}$ NMR spectrum. The molecular formula of complex **12** was also confirmed by HRMS ($m/z$ = 1545.2519).

Poly-oligo(ethylene glycol)methacrylates (POEGMAs) are very useful polymers, since they possess interesting thermoresponsive properties.[70–73] In this regard, we attempted the preparation of a co-polymer of POEGMA and our metalla-aromatic unit. As shown in Scheme 2, metallopolymer **13** was successfully prepared by single-electron transfer living radical polymerization (SET-LRP) of complex **12** and triethylene glycol methyl ether methacrylate (**14**) initiated by EBIB/Cu/Me$_6$TREN in DMF.[74,75] The organometallic substructure of **12** in metallopolymer **13** was confirmed by two signals observed at 10.99 and −18.09 ppm in the $^{31}P\{^{1}H\}$ NMR spectrum (Fig. S18†), which is similar to those of the monomer **12**. In the $^{1}H$ NMR spectrum of metallopolymer **13**, the presence of oligo(ethylene glycol) branches was confirmed by the signals located at 3.0–4.1 ppm and the presence of the polymethacrylate main chain was confirmed by the signals located at 0.8–2.0 ppm (Fig. S17†). These results indicated that our strategy to prepare the metal-containing copolymer **13** was successful. The unit ratio of **12/14** in metallopolymer **13** was calculated to be 1/26.0 by comparing the integral values of the aromatic protons (6.9–8.0 ppm) and H9 (3.27 ppm) in the $^{1}H$ NMR spectrum (Fig. S17†). By using the standard UV-Vis absorption curve of complex **10** (Fig. S22†), the unit ratio of **12/14** in metallopolymer **13** was calculated to be 1/21.4 based on the absorption value of **13** (0.3 mg mL$^{-1}$) at 605 nm (Fig. S23†). Both results are close to the polymerization feed ratio (1 : 20).

The molecular weight ($M_w$) and polydispersity index (PDI, $M_w/M_n$) of metallopolymer **13** were determined by size exclusion chromatography (SEC) in tetrahydrofuran (THF) to be $1.9 \times 10^4$ g mol$^{-1}$ and 1.20 (Fig. S19†), respectively. It is noted that the metallopolymer may feature a very different hydrodynamic radius versus the narrow polystyrene standards. For comparison, the $M_w$ and PDI of monomer **12** were also examined by the same SEC experiment to be $2.5 \times 10^3$ g mol$^{-1}$ and 1.00 (Fig. S25†), respectively.

To further estimate the molecular weight of metallopolymer **13**, we have tried to determine it by inverse gated $^{13}C\{^{1}H\}$ NMR spectroscopy. Based on the integral ratio (Fig. S19†) of the terminal ethoxy group (C17 from initiator) versus the methoxy (C9) group in the oligo ethylene glycol side-chains (repeating unit of **14**), the absolute molecular weight of metallopolymer **13** was calculated to be about 9500 with the help of the calculated ratio of **12/14** in metallopolymer **13**.

As expected, metallopolymer **13** presents good water solubility (3.0 mg mL$^{-1}$ in water), supporting the successful preparation of metallopolymer **13**. The most interesting feature of
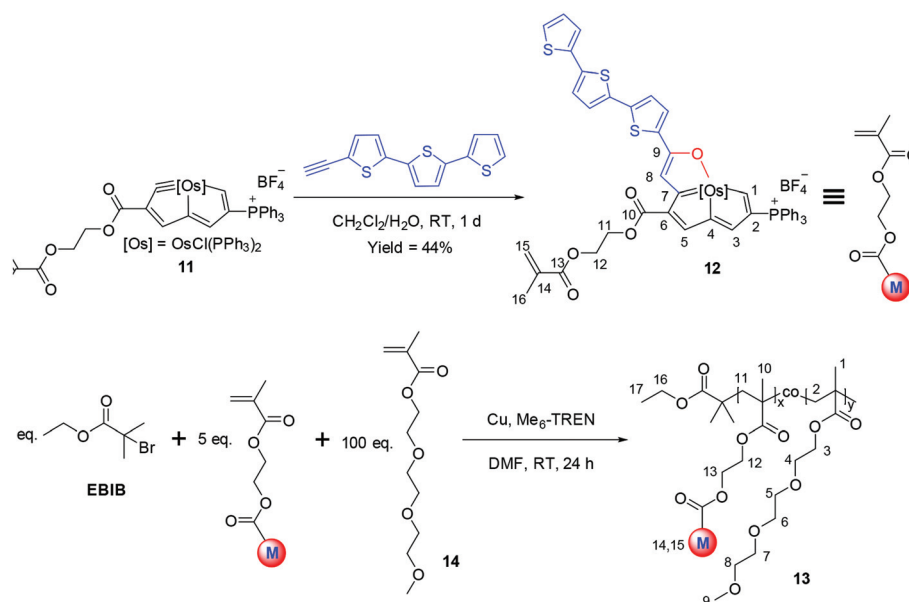


**Scheme 2** Synthesis of osmapentalenofuran **12** with the methacrylate group and metallopolymer **13**.
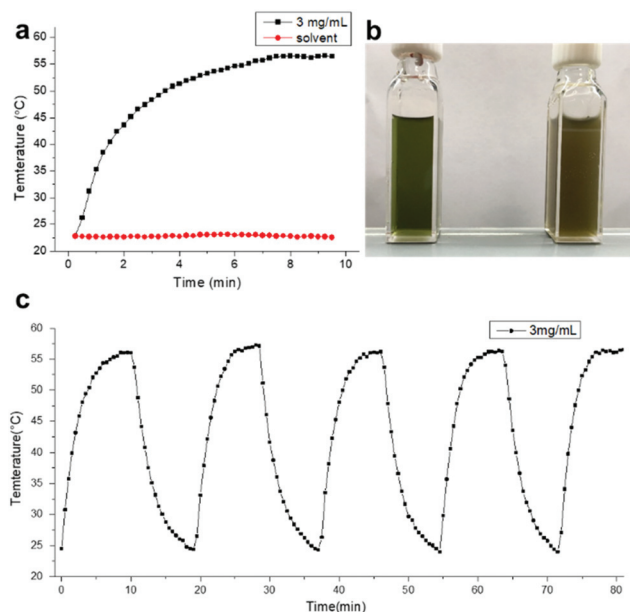
**Fig. 6** (a) Temperature curves of water (solvent) and a solution of metallopolymer **13** (3.0 mg mL$^{-1}$ in water) irradiated with an 808 nm laser at a power density of 1.0 W cm$^{-2}$. (b) Solutions of metallopolymer **13** in water before (left) and after (right) NIR irradiation. (c) Temperature curves of a solution of metallopolymer **13** (3.0 mg mL$^{-1}$ in water) irradiated with an 808 nm laser at a power density of 1.0 W cm$^{-2}$ with five laser on−off cycles.

metallopolymer **13** is its good photothermal property, as shown in Fig. 6. When a solution of metallopolymer **13** in water was irradiated with an NIR laser (808 nm, 1.0 W cm$^{-2}$), its temperature rose quickly from 22 to 56 °C in 8 min (Fig. 6(a)). In contrast, an increase in the temperature of water during the irradiation was negligible. As a result, the clear solution of **13** became turbid (Fig. 6(b)), indicating the occurrence of a phase transition. To further assess the NIR photostability of metallopolymer **13**, we have performed five laser on−off cycles (Fig. 6(c)). These results show that no significant change in an increase of the temperature was observed after five cycles, suggesting that metallopolymer **13** exhibit good photothermal stability under the laser irradiation conditions. It is noted that there are many NIR-responsive materials,[76] but pure NIR-responsive polymers[77–79] are rare. Thus, metallopolymer **13** represents a new NIR-responsive metal-containing copolymer, which has great potential applications as a small-molecule carrier with controlled release triggered by an NIR laser.

## Conclusions

In summary, we have successfully prepared metallapentalenofurans with oligothiophen-5-yl groups under very mild conditions. They are supported by NMR spectroscopy, HRMS, elemental analysis, single-crystal X-ray diffraction, and UV-vis-NIR absorption spectroscopy, as well as by time-dependent

DFT calculations. The Möbius aromatic metallapentalenofuran (**10**) bearing a terthiophene group showed a good photothermal effect induced by the *J*-aggregates. The temperature of its solution containing 1.00 mg mL$^{-1}$ of complex **10** in water–ethanol (1/9, v/v) would rise quickly from 28 to 57 °C within 5 min under an NIR irradiation (808 nm, 1.0 W cm$^{-2}$). Based on this observation, we prepared another photothermal metallapentalenofuran (**12**) containing a methacrylate group as a monomer. The monomer was also characterized by NMR spectroscopy, HRMS, and elemental analysis. Finally, this monomer was co-polymerized with oligo-(ethylene glycol) methacrylate to afford a new type of stimuli-responsive polymer (**13**), which was characterized by different NMR spectroscopy techniques and SEC measurements. The obtained metallopolymer showed both a thermal response and a NIR-light response. This new NIR-responsive metal-containing copolymer represents a new stimuli-responsive metallopolymer.

## Experimental

### General information

All syntheses were carried out under an inert atmosphere using standard Schlenk techniques unless otherwise stated. The starting material complex **5**,[1] 5-ethynyl-2,2′-bithiophene,[80] 5-ethynyl-2,2′:5′,2′-terthiophene,[80] and complex **11**[70] were synthesized according to the previously published literature. The other reagents and solvents were used as purchased from commercial sources without further purification. Column chromatography was performed on alumina gel (200–300 mesh) in air. Nuclear magnetic resonance (NMR) spectra were recorded on a Bruker AV-400 spectrometer (400 MHz), or a Bruker AV-500 spectrometer (500 MHz) at room temperature. $^1$H and $^{13}$C{$^1$H} NMR chemical shifts ($\delta$) are relative to tetramethylsilane, and $^{31}$P{$^1$H} NMR chemical shifts are relative to 85% H$_3$PO$_4$. The absolute values of the coupling constants are given in hertz (Hz). Multiplicities are abbreviated as s (singlet), d (doublet), t (triplet), m (multiplet) and br (broad). Elemental analysis (EA) data were collected on a Vario EL III elemental analyzer. The high-resolution mass spectral (HRMS) experiments were performed on a Bruker En Apex Ultra 7.0 T FT-MS. Absorption spectra were recorded on a Shimadzu UV2550 UV-Vis spectrophotometer. The relative molecular weights and molecular weight distribution were determined by size exclusion chromatography (SEC). The SEC system (Agilent 1100 Series) was equipped with a refractive-index detector and gel columns (PSS SDV 100 Å 3 μm and linear S 5 μm) maintained at 35 °C. Tetrahydrofuran was used as the eluent at a flow rate of 1.0 mL min$^{-1}$. The gel columns were calibrated with narrow-molecular-weight polystyrene standards (PDI ≤ 1.05, Shoko, Japan). The STL808T1-15W fiber-coupled laser system (Stone Company) was used in photothermal experiments and the temperature data were collected by using an FLIR A35 FOV 24 thermal imaging camera.

**Complex 8.** 2-Ethynylthiophene (80.2 μL, 0.80 mmol) was added to a solution of complex **5** (200 mg, 0.16 mmol) in 10 mL dichloromethane and 0.2 mL water in air. The mixture was stirred at room temperature (RT) for 1 d to afford a red solution. The solution was evaporated under vacuum to a volume of *ca.* 2 mL, and then was loaded on a neutral alumina column and eluted by the mixture of dichloromethane and acetone (5/1, v/v). The red band was collected, and the solvent was evaporated to dryness under vacuum to afford a red solid. Yield, 120 mg, 55%. $^1$H NMR plus $^1$H–$^{13}$C HSQC (500.2 MHz, CDCl$_3$): $\delta$ 13.75 (d, $J_{PH}$ = 15.3 Hz, 1H, H1), 8.00 (s, 1H, H8), 7.64 (s, 1H, H3, confirmed by $^1$H–$^{13}$C HSQC), 7.61 (s, 1H, H5, confirmed by $^1$H–$^{13}$C HSQC), 3.58 (s, 3H, COOC*H*$_3$), 7.95–6.95 ppm (48H, other aromatic protons). $^{31}$P NMR (202.5 MHz, CDCl$_3$): $\delta$ 10.75 (t, $J_{PP}$ = 3.9 Hz C*P*Ph$_3$), −17.38 ppm (d, $J_{PP}$ = 3.9 Hz Os*P*Ph$_3$). $^{13}$C NMR plus DEPT-135, $^1$H–$^{13}$C HSQC and $^1$H–$^{13}$C HMBC (125.8 MHz, CDCl$_3$): $\delta$ 224.9 (t, $J_{PC}$ = 6.2 Hz, C7), 208.5 (br, C1), 188.5 (s, C9), 181.1 (dt, $J_{PC}$ = 22.0 Hz, $J_{PC}$ = 4.5 Hz, C4), 168.0 (s, C5), 163.2 (s, *C*OOCH$_3$), 144.1 (d, $J_{PC}$ = 19.8 Hz, C3), 140.0 (s, C6), 120.6 (s, C8), 119.3 (d, $J_{PC}$ = 88.4 Hz, C2), 50.8 (s, COO*C*H$_3$), 140.5–124.9 ppm (other aromatic carbons). Elemental analysis calcd (%) for C$_{69}$H$_{55}$BClF$_4$O$_3$OsP$_3$S: C 60.51, H 4.05; found: C 60.63, H 4.30. HRMS (ESI): *m/z* calcd for [C$_{69}$H$_{55}$ClO$_3$OsP$_3$S]$^+$, 1283.2376; found, 1283.2377.

**Complex 9.** A solution of 5-ethynyl-2,2′-bithiophene (152 mg, 0.80 mmol) and complex **5** (200 mg, 0.16 mmol) in 10 mL dichloromethane and 0.2 mL water in air was stirred at RT for 1 d to afford a red solution. The solution was evaporated under vacuum to a volume of *ca.* 2 mL, and then was loaded on a neutral alumina column and eluted by the mixture of dichloromethane and acetone (4/1, v/v). The red band was collected, and the solvent was evaporated to dryness under vacuum to afford a red solid. Yield, 116 mg, 50%. $^1$H NMR plus $^1$H–$^{13}$C HSQC (400.1 MHz, CDCl$_3$): $\delta$ 13.72 (d, $J_{PH}$ = 14.9 Hz, 1H, H1), 7.96 (s, 1H, H8), 7.66 (s, 1H, H3, confirmed by $^1$H–$^{13}$C HSQC), 7.62 (s, 1H, H5, confirmed by $^1$H–$^{13}$C HSQC), 3.57 (s, 3H, COOC*H*$_3$), 7.85–7.00 ppm (50H, other aromatic protons). $^{31}$P NMR (162.0 MHz, CDCl$_3$): $\delta$ 10.79 (t, $J_{PP}$ = 3.9 Hz C*P*Ph$_3$), −17.41 ppm (d, $J_{PP}$ = 3.9 Hz Os*P*Ph$_3$). $^{13}$C NMR plus DEPT-135, $^1$H–$^{13}$C HSQC and $^1$H–$^{13}$C HMBC (100.6 MHz, CDCl$_3$): $\delta$ 224.4 (t, $J_{PC}$ = 5.9 Hz, C7), 208.6 (br, C1), 187.5 (s, C9), 181.1 (dt, $J_{PC}$ = 22.2 Hz, $J_{PC}$ = 4.1 Hz, C4), 168.3 (s, C5), 163.4 (s, *C*OOCH$_3$), 144.6 (d, $J_{PC}$ = 19.8 Hz, C3), 139.9 (s, C6), 120.4 (s, C8), 119.3 (d, $J_{PC}$ = 90.2 Hz, C2), 50.8 (s, COO*C*H$_3$), 145.5–124.2 ppm (other aromatic carbons). Elemental analysis calcd (%) for C$_{73}$H$_{57}$BClF$_4$O$_3$OsP$_3$S$_2$: C 60.39, H 3.96; found: C 60.62, H 3.88. HRMS (ESI): *m/z* calcd for [C$_{73}$H$_{57}$ClO$_3$OsP$_3$S$_2$]$^+$, 1365.2252; found, 1365.2274.

**Complex 10.** A solution of 5-ethynyl-2,2′:5′,2′-terthiophene (218 mg, 0.80 mmol) and complex **5** (200 mg, 0.16 mmol) in 10 mL dichloromethane and 0.2 mL water in air was stirred at RT for 1 d to afford a green solution. The solution was evaporated under vacuum to a volume of *ca.* 2 mL, and then was loaded on a neutral alumina column and eluted by the mixture of dichloromethane and acetone (3/1, v/v). The green

band was collected, and the solvent was evaporated to dryness under vacuum to afford a green solid. Yield, 118 mg, 48%. $^1$H NMR plus $^1$H–$^{13}$C HSQC (400.1 MHz, CDCl$_3$): $\delta$ 13.73 (d, $J_{PH}$ = 15.1 Hz, 1H, H1), 7.97 (s, 1H, H8), 7.69 (s, 1H, H3, confirmed by $^1$H–$^{13}$C HSQC), 7.64 (s, 1H, H5, confirmed by $^1$H–$^{13}$C HSQC), 3.57 (s, 3H, COOC*H*$_3$), 7.85–6.98 ppm (52H, other aromatic protons). $^{31}$P NMR (162.0 MHz, CDCl$_3$): $\delta$ 10.81 (t, $J_{PP}$ = 3.9 Hz C*P*Ph$_3$), −17.42 ppm (d, $J_{PP}$ = 3.9 Hz Os*P*Ph$_3$). $^{13}$C NMR plus DEPT-135, $^1$H–$^{13}$C HSQC and $^1$H–$^{13}$C HMBC (100.6 MHz, CDCl$_3$): $\delta$ 224.4 (t, $J_{PC}$ = 5.9 Hz, C7), 208.6 (br, C1), 187.3 (s, C9), 181.1 (dt, $J_{PC}$ = 22.4 Hz, $J_{PC}$ = 4.2 Hz, C4), 168.3 (s, C5), 163.4 (s, *C*OOCH$_3$), 144.7 (d, $J_{PC}$ = 19.8 Hz, C3), 139.9 (s, C6), 120.5 (s, C8), 119.3 (d, $J_{PC}$ = 89.8 Hz, C2), 50.8 (s, COO*C*H$_3$), 145.1–124.1 ppm (other aromatic carbons). Elemental analysis calcd (%) for C$_{77}$H$_{59}$BClF$_4$O$_3$OsP$_3$S$_3$: C 60.29, H 3.88; found: C 60.07, H 3.73. HRMS (ESI): *m/z* calcd for [C$_{77}$H$_{59}$ClO$_3$OsP$_3$S$_3$]$^+$, 1447.2128; found, 1447.2122.

**Complex 12.** A solution of 5-ethynyl-2,2′:5′,2′-terthiophene (218 mg, 0.80 mmol) and complex **11** (200 mg, 0.15 mmol) in 10 mL dichloromethane and 0.2 mL water in air was stirred at RT for 1 d to afford a green solution. The solution was evaporated under vacuum to a volume of *ca.* 2 mL, and then was loaded on a neutral alumina column and eluted by the mixture of dichloromethane and acetone (3/1, v/v). The green band was collected, and the solvent was evaporated to dryness under vacuum to afford a green solid. Yield: 107 mg, 44%. $^1$H NMR plus $^1$H–$^{13}$C HSQC (500.2 MHz, CDCl$_3$): $\delta$ 13.75 (d, $J_{PH}$ = 15.1 Hz, 1H, H1), 7.95 (s, 1H, H8), 7.65 (s, 1H, H3, confirmed by $^1$H–$^{13}$C HSQC), 7.59 (s, 1H, H5, confirmed by $^1$H–$^{13}$C HSQC), 6.23 (s, 1H, H15), 5.71 (s, 1H, H15), 4.36 (t, $J_{HH}$ = 4.7 Hz, 2H, H12), 4.23 (t, $J_{HH}$ = 4.7 Hz, 2H, H11), 2.02 (s, 3H, H16), 7.90–7.00 ppm (52H, other aromatic protons). $^{31}$P NMR (202.5 MHz, CDCl$_3$): $\delta$ 10.77 (s, C*P*Ph$_3$), −17.45 ppm (s, Os*P*Ph$_3$). $^{13}$C NMR plus DEPT-135, $^1$H–$^{13}$C HSQC and $^1$H–$^{13}$C HMBC (125.8 MHz, CDCl$_3$): $\delta$ 223.7 (br, C7), 209.0 (br, C1), 187.6 (s, C9), 181.1 (d, $J_{PC}$ = 21.5 Hz, C4), 168.1 (s, C5), 167.2 (s, C13), 162.5 (s, C10), 144.9 (d, $J_{PC}$ = 20.4 Hz, C3), 139.5 (s, C6), 136.0 (s, C14), 126.5 (s, C15), 120.6 (s, C8), 119.3 (d, $J_{PC}$ = 89.2 Hz, C2), 62.8 (s, C12), 61.9 (s, C11), 18.5 (s, C16), 145.4–124.1 ppm (other aromatic carbons). Elemental analysis, calcd (%) for C$_{82}$H$_{65}$BClF$_4$O$_5$OsP$_3$S$_3$: C 60.35, H 4.01; found: C 60.40, H 4.02. HRMS (ESI): *m/z* calcd for [C$_{82}$H$_{65}$ClO$_5$OsP$_3$S$_3$]$^+$, 1545.2505; found, 1545.2519.

**Metallopolymer 13.** An ampoule charged with ethyl-2-bromo-isobutanoate (EBIB, 6.6 μL, 0.044 mmol), tris[2-(dimethylamino)ethyl]amine (Me$_6$TREN, 3.2 μL, 0.012 mmol), complex **12** (341.5 mg, 0.22 mmol), triethylene glycol methyl ether methacrylate (1.0 mL, 4.42 mmol), and *N,N*-dimethyl formamide (DMF, 5 mL) was deaerated by three freeze–pump–thaw cycles in liquid N$_2$ and then sealed. A copper wire (*L* = 2 cm) was added to the mixture under a nitrogen atmosphere. The reaction mixture was stirred at RT for 24 h; then, 50 mL diethyl ether–hexane (1 : 5) was slowly poured into the mixture to afford a green precipitate, which was collected by filtration. The crude product was further purified by re-dissolving in dichloromethane (3 mL) and poured into diethyl ether (50 mL)

to afford a green solid. An analytically pure sample was thus obtained by repeating this procedure several times. Finally, the product was dried under vacuum to afford metallopolymer **13** as a green solid. Yield: 845.1 mg, 63%. $^1$H NMR (500.2 MHz, CD$_2$Cl$_2$): $\delta$ 13.62 (br, H15), 7.95–6.96 (aromatic protons in osmapentalenofuran units), 4.01 (br, 2H, H3, H12, and H13), 3.59–3.44 (10H, H4–H8), 3.27 (br, 3H, H9), 1.83–1.75 (2H, H2 and H11), 0.96–0.81 ppm (3H, H1 and H10). $^{31}$P NMR (202.5 MHz, CD$_2$Cl$_2$): $\delta$ 10.99 ppm (s, C$P$Ph$_3$), −18.09 (s, Os$P$Ph$_3$). SEC, $M_w$: 19 018 g mol$^{-1}$; $M_w/M_n$: 1.20.

**X-ray crystallographic analysis.** Single crystals suitable for X-ray diffraction were grown from a dichloromethane solution layered with hexane. Single-crystal X-ray diffraction data for **9** and **10** were collected on a Rigaku R-AXIS SPIDER IP CCD area detector with Mo Kα radiation ($\lambda$ = 0.71073 Å). Non-absorption corrections were applied to **9** and **10**. Using Olex2,[81] the structures of **9** and **10** were solved with the XS[82] structure solution program using the Patterson method and refined with the ShelXL[82] refinement package using least squares minimization. All non-hydrogen atoms were refined anisotropically unless otherwise stated. Hydrogen atoms were placed at idealized positions by assuming the riding model. Some of the solvent molecules and phenyl groups were disordered and refined with suitable restraints. CCDC 1814896 (**9**) and 1814898 (**10**)† contain the supplementary crystallographic data for this paper.

**Crystal data for complex 9.** C$_{75}$H$_{61}$BCl$_5$F$_4$O$_3$OsP$_3$S$_2$ [C$_{73}$H$_{57}$ClO$_3$OsP$_3$S$_2$]BF$_4$·2CH$_2$Cl$_2$ ($M_r$ = 1621.52 g mol$^{-1}$): monoclinic, crystal dimension 0.10 × 0.10 × 0.10 mm, space group $P2_1/c$ (no. 14), $a$ = 24.7978(6) Å, $b$ = 14.1129(3) Å, $c$ = 20.1547(4) Å, $\beta$ = 96.6450(10)°, $V$ = 7006.1(3) Å$^3$, $Z$ = 4, $T$ = 173 K, $\mu$(MoKα) = 2.198 mm$^{-1}$, $D_{calc.}$ = 1.537 g mm$^{-3}$, 102 445 reflections measured (6.006 ≤ 2$\Theta$ ≤ 54.966), 16 024 unique ($R_{int}$ = 0.1045, $R_{sigma}$ = 0.0676), which were used in all calculations. The final $R_1$ was 0.0503 ($I > 2\sigma(I)$) and w$R_2$ was 0.1469 (all data). GOF = 1.110. Residual electron density (e Å$^{-3}$) max/min: 2.38/−2.72.

**Crystal data for complex 10.** C$_{77}$H$_{59}$BClF$_4$O$_3$OsP$_3$S$_3$ [C$_{77}$H$_{59}$ClO$_3$OsP$_3$S$_3$]BF$_4$ ($M_r$ = 1533.79 g mol$^{-1}$): triclinic, crystal dimension 0.25 × 0.20 × 0.20 mm, space group $P\bar{1}$ (no. 2), $a$ = 11.1803(3) Å, $b$ = 14.1709(4) Å, $c$ = 23.4379(6) Å, $\alpha$ = 76.6530 (10)°, $\beta$ = 84.0290(10)°, $\gamma$ = 69.3370(10)°, $V$ = 3379.62(16) Å$^3$, $Z$ = 2, $T$ = 173 K, $\mu$(MoKα) = 2.150 mm$^{-1}$, $D_{calc.}$ = 1.507 g mm$^{-3}$, 54 869 reflections measured (6.016 ≤ 2$\Theta$ ≤ 54.968), 15 481 unique ($R_{int}$ = 0.0842, $R_{sigma}$ = 0.0775), which were used in all calculations. The final $R_1$ was 0.0626 ($I > 2\sigma(I)$) and w$R_2$ was 0.1752 (all data). GOF = 1.031. Residual electron density (e Å$^{-3}$) max/min: 1.57/−2.82.

**Computational details.** All the calculations were performed with the Gaussian 09 software package.[83] The B3LYP/6-31G** level[84–86] of density functional theory was used to optimize all the structures studied in this work. In the B3LYP calculations, the effective core potentials (ECPs) of Hay and Wadt with a double-ζ valence basis set (LanL2DZ) were used to describe Os, S, and P atoms, whereas the standard 6-31G** basis set was used for C, O, and H atoms.[87] Polarization functions were added for Os ($\zeta$(f) = 0.886), S ($\zeta$(d) = 0.421), and P ($\zeta$(d) =

0.340).[88] We calculated the UV-Vis absorption spectra of the cationic part of **8**, **9**, and **10** using the PCM model with dichloromethane as the solvent.

## Conflicts of interest

There are no conflicts to declare.

## Acknowledgements

## References

1 C. Zhu, S. Li, M. Luo, X. Zhou, Y. Niu, M. Lin, J. Zhu, Z. Cao, X. Lu, T. Wen, Z. Xie, P. V. Schleyer and H. Xia, *Nat. Chem.*, 2013, **5**, 698–703.

2 C. Zhu, M. Luo, Q. Zhu, J. Zhu, P. V. Schleyer, J. I. Wu, X. Lu and H. Xia, *Nat. commun.*, 2014, **5**, 3265.

3 C. Zhu, C. Yang, Y. Wang, G. Lin, Y. Yang, X. Wang, J. Zhu, X. Chen, X. Lu, G. Liu and H. Xia, *Sci. Adv.*, 2016, **2**, e1601031.

4 Z. Lu, C. Zhu, Y. Cai, J. Zhu, Y. Hua, Z. Chen, J. Chen and H. Xia, *Chem. – Eur. J.*, 2017, **23**, 6426–6431.

5 C. Zhu, Y. Yang, M. Luo, C. Yang, J. Wu, L. Chen, G. Liu, T. Wen, J. Zhu and H. Xia, *Angew. Chem., Int. Ed.*, 2015, **54**, 6181–6185.

6 C. Yang, G. Lin, C. Zhu, X. Pang, Y. Zhang, X. Wang, X. Li, B. Wang, H. Xia and G. Liu, *J. Mater. Chem. B*, 2018, DOI: 10.1039/C7TB02145C.

7 X. He, X. He, S. Li, K. Zhuo, W. Qin, S. Dong, J. Chen, L. Ren, G. Liu and H. Xia, *Polym. Chem.*, 2017, **8**, 3674–3678.

8 P. Nguyen, P. Gomez-Elipe and I. Manners, *Chem. Rev.*, 1999, **99**, 1515–1548.

9 I. Manners, *Science*, 2001, **294**, 1664–1666.

10 J.-C. Eloi, L. Chabanne, G. R. Whittell and I. Manners, *Mater. Today*, 2008, **11**, 28–36.

11 L. Zhao, X. Liu, L. Zhang, G. Qiu, D. Astruc and H. Gu, *Coord. Chem. Rev.*, 2017, **337**, 34–79.

12 R. Pietschnig, *Chem. Soc. Rev.*, 2016, **45**, 5216–5231.

13 Y. Yan, J. Zhang, L. Ren and C. Tang, *Chem. Soc. Rev.*, 2016, **45**, 5232–5263.

14 C.-L. Ho, Z.-Q. Yu and W.-Y. Wong, *Chem. Soc. Rev.*, 2016, **45**, 5264–5295.

15 A. Winter and U. S. Schubert, *Chem. Soc. Rev.*, 2016, **45**, 5311–5357.

16 R. L. N. Hailes, A. M. Oliver, J. Gwyther, G. R. Whittell and I. Manners, *Chem. Soc. Rev.*, 2016, **45**, 5358–5407.

17 J. M. Stanley and B. J. Holliday, *Coord. Chem. Rev.*, 2012, **256**, 1520–1530.

18 G. R. Whittell, M. D. Hager, U. S. Schubert and I. Manners, *Nat. Mater.*, 2011, **10**, 176–188.

19 C.-L. Ho and W.-Y. Wong, *Coord. Chem. Rev.*, 2011, **255**, 2469–2502.

20 A. S. Abd-El-Aziz, P. O. Shipman, B. N. Boden and W. S. McNeil, *Prog. Polym. Sci.*, 2010, **35**, 714–836.

21 J. Liu, J. W. Y. Lam and B. Z. Tang, *Chem. Rev.*, 2009, **109**, 5799–5867.

22 D. Scheid, M. von der Luehe and M. Gallei, *Macromol. Rapid Commun.*, 2016, **37**, 1573–1580.

23 W. Zhang, J. Zhu, H. Ang, H. Wang, H. T. Tan, D. Yang, C. Xu, N. Xiao, B. Li, W. Liu, X. Wang, H. H. Hng and Q. Yan, *ACS Appl. Mater. Interfaces*, 2014, **6**, 7164–7170.

24 C. Zhao, S. Sun, W.-L. Tong and M. C. W. Chan, *Macromolecules*, 2017, **50**, 6896–6902.

25 J. Li, H. Ejima and N. Yoshie, *ACS Appl. Mater. Interfaces*, 2016, **8**, 19047–19053.

26 J. Zhang, J. Yan, P. Pageni, Y. Yan, A. Wirth, Y. Qiao, Q. Wang, C. Tang, Y.-P. Chen and A. W. Decho, *Sci. Rep.*, 2015, **5**, 11914.

27 S. Nagappan, S. S. Park, E. J. Yu, H. J. Cho, J. J. Park, W.-K. Lee and C.-S. Ha, *J. Mater. Chem. A*, 2013, **1**, 12144–12153.

28 S. Bode, M. Enke, R. K. Bose, F. H. Schacher, S. J. Garcia, S. van der Zwaag, M. D. Hager and U. S. Schubert, *J. Mater. Chem. A*, 2015, **3**, 22145–22153.

29 R. S. Vishwanath and S. Kandaiah, *J. Mater. Chem. A*, 2017, **5**, 2052–2065.

30 E. Degtyar, M. J. Harrington, Y. Politi and P. Fratzl, *Angew. Chem., Int. Ed.*, 2014, **53**, 12026–12044.

31 J. Xiang, C.-L. Ho and W.-Y. Wong, *Polym. Chem.*, 2015, **6**, 6905–6930.

32 D. P. Puzzo, A. C. Arsenault, I. Manners and G. A. Ozin, *Angew. Chem., Int. Ed.*, 2009, **48**, 943–947.

33 X. Feng, X. Sui, M. A. Hempenius and G. J. Vancso, *J. Am. Chem. Soc.*, 2014, **136**, 7865–7868.

34 T. Gaedt, N. S. Ieong, G. Cambridge, M. A. Winnik and I. Manners, *Nat. Mater.*, 2009, **8**, 144–150.

35 Z. M. Hudson, C. E. Boott, M. E. Robinson, P. A. Rupar, M. A. Winnik and I. Manners, *Nat. Chem.*, 2014, **6**, 893–898.

36 H. Qiu, Y. Gao, C. E. Boott, O. E. C. Gould, R. L. Harniman, M. J. Miles, S. E. D. Webb, M. A. Winnik and I. Manners, *Science*, 2016, **352**, 697–701.

37 C. Zhu, Q. Zhu, J. Fan, J. Zhu, X. He, X. Y. Cao and H. Xia, *Angew. Chem., Int. Ed.*, 2014, **53**, 6232–6236.

38 C. Zhu, Y. Yang, J. Wu, M. Luo, J. Fan, J. Zhu and H. Xia, *Angew. Chem., Int. Ed.*, 2015, **54**, 7189–7192.

39 C. Zhu, X. Zhou, H. Xing, K. An, J. Zhu and H. Xia, *Angew. Chem., Int. Ed.*, 2015, **54**, 3102–3106.

40 M. Luo, C. Zhu, L. Chen, H. Zhang and H. Xia, *Chem. Sci.*, 2016, **7**, 1815–1818.

41 M. Luo, L. Long, H. Zhang, Y. Yang, Y. Hua, G. Liu, Z. Lin and H. Xia, *J. Am. Chem. Soc.*, 2017, **139**, 1822–1825.

42 C. Zhu, J. Wu, S. Li, Y. Yang, J. Zhu, X. Lu and H. Xia, *Angew. Chem., Int. Ed.*, 2017, **56**, 9067–9071.

43 H. Wang, X. Zhou and H. Xia, *Chin. J. Chem.*, 2018, **36**, 93–105.

44 T. T. Tidwell, *Angew. Chem., Int. Ed.*, 2001, **40**, 331–337.

45 D. Möbius, *Adv. Mater.*, 1995, **7**, 437–444.

46 A. Mishra, R. K. Behera, P. K. Behera, B. K. Mishra and G. B. Behera, *Chem. Rev.*, 2000, **100**, 1973–2012.

47 F. Würthner, T. E. Kaiser and C. R. Saha-Möller, *Angew. Chem., Int. Ed.*, 2011, **50**, 3376–3410.

48 D. Zhai, W. Xu, L. Zhang and Y.-T. Chang, *Chem. Soc. Rev.*, 2014, **43**, 2402–2411.

49 N. J. Hestand and F. C. Spano, *Acc. Chem. Res.*, 2017, **50**, 341–350.

50 S. E. Skrabalak, J. Chen, Y. Sun, X. Lu, L. Au, C. M. Cobley and Y. Xia, *Acc. Chem. Res.*, 2008, **41**, 1587–1595.

51 S. Lal, S. E. Clare and N. J. Halas, *Acc. Chem. Res.*, 2008, **41**, 1842–1851.

52 E. Boisselier and D. Astruc, *Chem. Soc. Rev.*, 2009, **38**, 1759–1782.

53 R. Bardhan, S. Lal, A. Joshi and N. J. Halas, *Acc. Chem. Res.*, 2011, **44**, 936–946.

54 Y. Xia, W. Li, C. M. Cobley, J. Chen, X. Xia, Q. Zhang, M. Yang, E. C. Cho and P. K. Brown, *Acc. Chem. Res.*, 2011, **44**, 914–924.

55 K. Yang, L. Feng, X. Shi and Z. Liu, *Chem. Soc. Rev.*, 2013, **42**, 530–547.

56 L. Cheng, C. Wang, L. Feng, K. Yang and Z. Liu, *Chem. Rev.*, 2014, **114**, 10869–10939.

57 H. Dong, S.-R. Du, X.-Y. Zheng, G.-M. Lyu, L.-D. Sun, L.-D. Li, P.-Z. Zhang, C. Zhang and C.-H. Yan, *Chem. Rev.*, 2015, **115**, 10725–10815.

58 X. Yang, M. Yang, B. Pang, M. Vara and Y. Xia, *Chem. Rev.*, 2015, **115**, 10410–10488.

59 J. Fabian, H. Nakazumi and M. Matsuoka, *Chem. Rev.*, 1992, **92**, 1197–1226.

60 G. Qian and Z. Y. Wang, *Chem. – Asian J.*, 2010, **5**, 1006–1029.

61 L. Xu, L. Cheng, C. Wang, R. Peng and Z. Liu, *Polym. Chem.*, 2014, **5**, 1573–1580.

62 X. Song, Q. Chen and Z. Liu, *Nano Res.*, 2015, **8**, 340–354.

63 X. Song, H. Gong, T. Liu, L. Cheng, C. Wang, X. Sun, C. Liang and Z. Liu, *Small*, 2014, **10**, 4362–4370.

64 X. Song, R. Zhang, C. Liang, Q. Chen, H. Gong and Z. Liu, *Biomaterials*, 2015, **57**, 84–92.

65 Y. Deng, L. Huang, H. Yang, H. Ke, H. He, Z. Guo, T. Yang, A. Zhu, H. Wu and H. Chen, *Small*, 2017, **13**, 1602747.

66 L. Feng, D. Tao, Z. Dong, Q. Chen, Y. Chao, Z. Liu and M. Chen, *Biomaterials*, 2017, **127**, 13–24.

67 H. He, S. Ji, Y. He, A. Zhu, Y. Zou, Y. Deng, H. Ke, H. Yang, Y. Zhao, Z. Guo and H. Chen, *Adv. Mater.*, 2017, **29**, 1606690.

68 S. Shen, Y. Chao, Z. Dong, G. Wang, X. Yi, G. Song, K. Yang, Z. Liu and L. Cheng, *Adv. Funct. Mater.*, 2017, **27**, 1700250.

69 K. Matyjaszewski and T. P. Davis, *Handbook of Radical Polymerization*, John Wiley & Sons, Inc., 2003.

70 Z. Lu, J. Chen and H. Xia, *Chin. J. Org. Chem.*, 2017, **37**, 1181–1188.

71 J.-F. Lutz, Ö. Akdemir and A. Hoth, *J. Am. Chem. Soc.*, 2006, **128**, 13046–13047.

72 Z.-B. Hu, T. Cai and C.-L. Chi, *Soft Matter*, 2010, **6**, 2115–2123.

73 G. Vancoillie, D. Frank and R. Hoogenboom, *Prog. Polym. Sci.*, 2014, **39**, 1074–1095.

74 V. Percec, T. Guliashvili, J. S. Ladislaw, A. Wistrand, A. Stjerndahl, M. J. Sienkowska, M. J. Monteiro and S. Sahoo, *J. Am. Chem. Soc.*, 2006, **128**, 14156–14165.

75 B. M. Rosen and V. Percec, *Chem. Rev.*, 2009, **109**, 5069–5119.

76 X. Huang, W. Zhang, G. Guan, G. Song, R. Zou and J. Hu, *Acc. Chem. Res.*, 2017, **50**, 2529–2538.

77 P. Weis and S. Wu, *Macromol. Rapid Commun.*, 2018, **39**, 1700220.

78 G. Uğur, J. Chang, S. Xiang, L. Lin and J. Lu, *Adv. Mater.*, 2012, **24**, 2685–2690.

79 Y. Dai, H. Sun, S. Pal, Y. Zhang, S. Park, C. P. Kabb, W. D. Wei and B. S. Sumerlin, *Chem. Sci.*, 2017, **8**, 1815–1821.

80 X. Zhao, C. Piliego, B. Kim, D. A. Poulsen, B. Ma, D. A. Unruh and J. M. J. Fréchet, *Chem. Mater.*, 2010, **22**, 2325–2332.

81 O. V. Dolomanov, L. J. Bourhis, R. J. Gildea, J. A. K. Howard and H. Puschmann, *J. Appl. Crystallogr.*, 2009, **42**, 339–341.

82 G. M. Sheldrick, *Acta Crystallogr., Sect. A: Found. Crystallogr.*, 2008, **64**, 112–122.

83 M. J. Frisch, G. W. Trucks, H. B. Schlegel, G. E. Scuseria, M. A. Robb, J. R. Cheeseman, G. Scalmani, V. Barone, B. Mennucci, G. A. Petersson, H. Nakatsuji, M. Caricato, X. Li, H. P. Hratchian, A. F. Izmaylov, J. Bloino, G. Zheng, J. L. Sonnenberg, M. Hada, M. Ehara, K. Toyota, R. Fukuda, J. Hasegawa, M. Ishida, T. Nakajima, Y. Honda, O. Kitao, H. Nakai, T. Vreven, J. A. Montgomery Jr., J. E. Peralta, F. Ogliaro, M. Bearpark, J. J. Heyd, E. Brothers, K. N. Kudin, V. N. Staroverov, T. Keith, R. Kobayashi, J. Normand, K. Raghavachari, A. Rendell, J. C. Burant, S. S. Iyengar, J. Tomasi, M. Cossi, N. Rega, J. M. Millam, M. Klene, J. E. Knox, J. B. Cross, V. Bakken, C. Adamo, J. Jaramillo, R. Gomperts, R. E. Stratmann, O. Yazyev, A. J. Austin, R. Cammi, C. Pomelli, J. W. Ochterski, R. L. Martin, K. Morokuma, V. G. Zakrzewski, G. A. Voth, P. Salvador, J. J. Dannenberg, S. Dapprich, A. D. Daniels, O. Farkas, J. B. Foresman, J. V. Ortiz, J. Cioslowski and D. J. Fox, *Gaussian 09, Revision D.01*, Gaussian, Inc., Wallingford CT, 2013.

84 C. Lee, W. Yang and R. G. Parr, *Phys. Rev. B: Condens. Matter Mater. Phys.*, 1988, **37**, 785–789.

85 B. Miehlich, A. Savin, H. Stoll and H. Preuss, *Chem. Phys. Lett.*, 1989, **157**, 200–206.

86 A. D. Becke, *J. Chem. Phys.*, 1993, **98**, 5648–5652.

87 P. J. Hay and W. R. Wadt, *J. Chem. Phys.*, 1985, **82**, 299–310.

88 S. Huzinaga, *Gaussian Basis Sets for Molecular Calculations*, Elsevier Science Pub. Co., Amsterdam, 1984.